Stochastic Volatility Effects on Defaultable Bonds

Jean-Pierre Fouque* Ronnie Sircar† Knut Sølna‡

December 2004; revised October 24, 2005

Abstract

We study the effect of introducing stochastic volatility in the first passage structural approach to default risk. We analyze the impact of volatility time scales on the yield spread curve. In particular we show that the presence of a short time scale in the volatility raises the yield spreads at short maturities. We argue that combining first passage default modeling with multiscale stochastic volatility produces more realistic yield spreads. Moreover this framework enables us to use perturbation techniques to derive explicit approximations which facilitate the complicated issue of calibration of parameters.

Contents

*Department of Mathematics, NC State University, Raleigh NC 27695-8205, *fouque@math.ncsu.edu*. Work supported by NSF grant DMS-0455982

†Department of Operations Research & Financial Engineering, Princeton University, E-Quad, Princeton, NJ 08544, *sircar@princeton.edu*. Work partially supported by NSF grants DMS-0306357 and DMS-0456195.

‡Department of Mathematics, University of California, Irvine CA 92697, *ksolna@math.uci.edu*.

1 Introduction

In this paper, we revisit the first passage structural approach to default. This model supposes that a defaultable zero-coupon bond written on a risky asset X is a bond which pays \$1 at maturity T if the asset price X_t stays above a given default threshold $B > 0$, and pays nothing if X_t goes below B at some time before maturity. It is well documented in the literature that in this first passage model, yield spreads go to zero with the maturity, which is in contradiction to observed data. This is illustrated in Figure 1 in the case of highly levered firms, corresponding to X_0/B close to one. For a general introduction to *Credit Risk*, including other approaches to default, such as the intensity based reduced form models, we refer for instance to the books [1], [5], and [22]. An introduction can also be found in [16] along with other contributions in the book [23].

As stated by Eom *et al.* [8], one of the challenges for theoretical pricing models is to raise the average predicted spread relative to crude models such as the constant volatility model presented in the next section, without overstating the risks associated with volatility or leverage. Several approaches have been proposed that aim at improving modeling in this regard. These include the introduction of jumps, [3, 17, 25], stochastic interest rates [20], or imperfect information on X [5, 7]. Another interesting approach is taken in [14] where uncertainty is introduced on the default threshold.

In this paper, we propose to handle this challenge by introducing stochastic volatility in the dynamics of the defaultable asset, and using the framework of multiscale stochastic volatility developed in the context of equity markets [9, 10, 12] and interest-rate derivatives [6].

1.1 Defaultable Bonds

Assuming that the underlying is traded, the classical arbitrage free value of a defaultable bond is the expected value of its discounted payoff computed with respect to a risk neutral measure $I\!P^\star$, under which the discounted asset price is a martingale. The market may be incomplete and we adopt here the point of view that $I\!P^\star$ is selected by the market among the possible risk neutral pricing measures.

Our focus is on the effect of stochastic volatility, and we study the simplest first-passage model, as introduced by Black-Cox [2] with constant volatility. In the detailed analysis, we assume zero recovery on default, but we remark on extension to some loss recovery models in Section 2, with the generalized boundary condition (10). If the risk free interest rate r is constant, the value of this bond at time $t \leq T$, denoted by $\Gamma^B(t,T)$, is given by

$$\begin{aligned} \Gamma^B(t,T) &= I\!E^\star \left\{ e^{-r(T-t)} \mathbf{1}_{\{\inf_{0\leq s\leq T} X_s > B\}} \mid \mathcal{F}_t \right\} \\ &= \mathbf{1}_{\{\inf_{0\leq s\leq t} X_s > B\}} e^{-r(T-t)} I\!E^\star \left\{ \mathbf{1}_{\{\inf_{t\leq s\leq T} X_s > B\}} \mid \mathcal{F}_t \right\}, \end{aligned} \tag{1}$$

where we denote the expected value with respect to $I\!P^\star$ by $I\!E^\star$, and the history of the dynamics up to time t by $\mathcal{F}_t$. Indeed $\Gamma^B(t,T) = 0$ if the asset price has reached B before time t, which is reflected by the factor $\mathbf{1}_{\{\inf_{0\leq s\leq t} X_s > B\}}$. This defaultable zero-coupon bond is in fact a *binary down-and-out barrier option* where the barrier level and the strike price coincide.

Introducing the default time τ_t defined by $\tau_t = \inf\{s \geq t, X_s \leq B\}$, one has

$$I\!E^\star \left\{ \mathbf{1}_{\{\inf_{t\leq s\leq T} X_s > B\}} \mid \mathcal{F}_t \right\} = I\!P^\star\{\tau_t > T \mid \mathcal{F}_t\},$$

which shows that the problem reduces to the characterization of the distribution of first-passage times. Observe that in the case of a continuous diffusion process X_t, the default time τ_t is a *predictable* stopping time, in the sense that it can be *announced* by an increasing sequence of stopping times. For instance one can consider the sequence $(\tau_t^{(n)})$ defined by $\tau_t^{(n)} = \inf\{s \geq t, X_s \leq B + 1/n\}$. As shown in [15, Theorem 3.1], this implies that yield spreads converge to zero with maturity. Our approach using stochastic volatility and, in particular, multiscale models, allows to conveniently control the *rate* of convergence of the spreads, and raise the predicted spreads at short maturities.

1.2 Outline of the Paper

In Section 2, we briefly recall the derivation of Merton, and Black and Cox pricing formulas (2) and (8) in the case where the underlying X_t follows a geometric Brownian motion with constant volatility. This leads to the explicit formula (12) for the yield spreads.

In Section 3, we consider the case where volatility is driven by an additional mean-reverting stochastic factor. In this case, there is no explicit formula for the yield spreads and we study

by Monte Carlo simulations the effect of stochastic volatility on the yield spread curve and, in particular, the effects of volatility *time scales*. For a long time scale, corresponding to slowly varying volatility, we observe a weak effect on long maturities and a negligible effect on short maturities. A volatility time scale of order one has an effect comparable to raising the volatility level and does not significantly affect short maturities. However a short time scale, corresponding to fast mean-reverting volatility, produces a significant increase of spreads at short maturities. We therefore argue that modeling with a fast stochastic volatility time scale is efficient for handling the main challenge of raising spreads at short maturities, while an additional slow scale provides flexibility in capturing long maturity spreads (see Figure 9 for an example).

In Section 4, we carry out a singular perturbation analysis which enables us to obtain the explicit approximation (34) to the price of a defaultable bond when volatility is fast mean-reverting. The case with a slowly mean-reverting stochastic volatility gives rise to a regular perturbation problem which we analyze in Section 5. The corresponding explicit price approximation is given in (47). In Section 6, we consider a class of multiscale stochastic volatility models which we analyze by combining singular and regular perturbation techniques. We show that our explicit formulas for the approximated prices, involving a few group market parameters, facilitate the essential calibration step, which is demonstrated with market data in Section 7.

2 The Constant Volatility Case

We first recall how the price of a defaultable zero-coupon bond is computed in the Black-Scholes model

$$dX_t \;=\; \mu X_t dt + \sigma X_t dW_t,$$

with a constant volatility σ and no dividend. In this case, under the unique risk neutral measure $I\!P^\star$, the asset price is explicitly given by

$$X_t \;=\; X_0 \exp\left((r - \frac{1}{2}\sigma^2)t + \sigma W_t^\star\right),$$

where $W^\star$ is a $I\!P^\star$-Brownian motion.

In the Merton [21] approach, default occurs if $X_T < B$ for some threshold value B. In this case, the price at time t of a defaultable bond is simply the price of a European digital option which pays one if X_T exceeds the threshold and zero otherwise. It is explicitly given by $u^d(t, X_t)$, where

$$\begin{aligned} u^d(t,x) &= I\!E^\star\left\{e^{-r(T-t)}\mathbf{1}_{\{X_T>B\}} \mid X_t = x\right\} \\ &= e^{-r(T-t)}N(d_2(T-t)), \end{aligned} \tag{2}$$

with the *distance to default* d_2 defined by:

$$d_2(T-t) \;=\; \frac{\log\left(\frac{x}{B}\right) + \left(r - \frac{\sigma^2}{2}\right)(T-t)}{\sigma\sqrt{T-t}}. \tag{3}$$

In the Black and Cox generalization [2], the default occurs the first time the underlying hits the threshold B as described in Section 1.1. From a probabilistic point of view, we have

$$\begin{aligned} & I\!E^\star \left\{ \mathbf{1}_{\{\inf_{t\le s\le T} X_s > B\}} \mid \mathcal{F}_t \right\} \\ = \; & I\!P^\star \left\{ \inf_{t\le s\le T} \left((r - \frac{\sigma^2}{2})(s-t) + \sigma(W_s^\star - W_t^\star) \right) > \log\left(\frac{B}{x}\right) \mid X_t = x \right\}, \end{aligned}$$

which can be computed by using the distribution of the minimum of a (non standard) Brownian motion. From the point of view of partial differential equations, we have

$$I\!E^\star \left\{ e^{-r(T-t)} \mathbf{1}_{\{\inf_{t\le s\le T} X_s > B\}} \mid \mathcal{F}_t \right\} \;=\; u_{BS}(t, X_t; \sigma),$$

where $u_{BS}(t,x;\sigma)$ is the solution of the following problem

$$\begin{aligned} & \mathcal{L}_{BS}(\sigma) u_{BS} = 0 \text{ on } x > B,\, t < T \\ & u_{BS}(t, B; \sigma) = 0 \quad \text{for } t \le T \\ & u_{BS}(T, x; \sigma) = 1 \text{ for } x > B. \end{aligned} \tag{4}$$

Here, $\mathcal{L}_{BS}(\sigma)$ denotes the Black-Scholes partial differential operator at volatility level σ:

$$\mathcal{L}_{BS}(\sigma) = \frac{\partial}{\partial t} + \frac{1}{2}\sigma^2 x^2 \frac{\partial^2}{\partial x^2} + r\left(x\frac{\partial}{\partial x} - \cdot \right). \tag{5}$$

This problem can be solved by introducing the solution $u^d(t,x)$ of the corresponding digital option problem

$$\begin{aligned} & \mathcal{L}_{BS}(\sigma) u^d = 0 \text{ on } x > 0,\, t < T \\ & u^d(T, x) = \mathbf{1}_{\{x>B\}}. \end{aligned} \tag{6}$$

The price of this European digital option is given by $u^d(t, X_t)$ at time $t < T$, where $u^d(t,x)$ is computed explicitly in (2). It can be checked that the solution $u_{BS}(t,x;\sigma)$ of the problem (4) can be written

$$u_{BS}(t,x;\sigma) \;=\; u^d(t,x) - \left(\frac{x}{B}\right)^{1-\frac{2r}{\sigma^2}} u^d\left(t, \frac{B^2}{x}\right). \tag{7}$$

This formula can be obtained by the method of images presented for instance in [24].

We combine the expression (2) for $u^d(t,x)$ with (7), to obtain

$$u_{BS}(t,x;\sigma) \;=\; e^{-r(T-t)} \left(N(d_2^+(T-t)) - \left(\frac{x}{B}\right)^{1-\frac{2r}{\sigma^2}} N(d_2^-(T-t)) \right), \tag{8}$$

$$d_2^\pm(T-t) \;=\; \frac{\pm \log\left(\frac{x}{B}\right) + \left(r - \frac{\sigma^2}{2}\right)(T-t)}{\sigma\sqrt{T-t}}. \tag{9}$$

Remark: This framework can be adapted for constant or time-dependent deterministic recovery on default by changing the boundary condition at $x = B$ in equation (4) to

$$u(t, B; \sigma) = q(t), \tag{10}$$

where q is the recovery function. Such non-homogeneous boundary value problems arise in the computation of the stochastic volatility correction (see Section 4.2, equation (26)) and we present the technique to handle them there. However, we will not explicitly address recovery models here.

Recall that the *yield spread* $Y(0,T)$ at time zero is defined by

$$e^{-Y(0,T)T} = \frac{\Gamma^B(0,T)}{\Gamma(0,T)}, \tag{11}$$

where $\Gamma(0,T)$ is the default free zero-coupon bond price given here, in the case of constant interest rate r, by $\Gamma(0,T) = e^{-rT}$, and $\Gamma^B(0,T) = u_{BS}(0,x;\sigma)$. Notice that the term-structure notation $\Gamma^B(t,T)$ shows the current and maturity times, while the pricing function $u_{BS}(t,x;\sigma)$ shows the current time, current level of the underlying and the volatility. We thus obtain the formula

$$Y(0,T) = -\frac{1}{T}\log\left(N\left(d_2^+(T)\right) - \left(\frac{x}{B}\right)^{1-\frac{2r}{\sigma^2}} N\left(d_2^-(T)\right)\right). \tag{12}$$

In Figure 1, we show in the left plot the yield spread curve $Y(0,T)$ as a function of maturity T for some typical values of the constant volatility, the other parameters are the constant interest rate r and the ratio of initial value to default level x/B. It is well documented in the literature that in this first passage model, the likelihood of default is essentially zero for short maturities even for highly levered firms, corresponding to B/x close to one, as illustrated in the plots on the right of Figure 1. As discussed in the introduction, the challenge for theoretical pricing models is to raise the average predicted spread relative to crude models such as the constant volatility model presented in this section, without overstating the risks associated with volatility or leverage.

In this paper, we propose to handle this challenge by introducing stochastic volatility in the dynamics of the defaultable asset. We explain in the following sections that a naive introduction of stochastic volatility may not modify the credit spreads significantly. However, a careful modeling of the time scale content of the volatility gives the desired modification in the yield spread at short maturities.

3 Stochastic Volatility

3.1 A Class of Models

In the context of equity markets and derivatives pricing and hedging, stochastic volatility is recognized as an essential feature in the modelling of the underlying dynamics. For an extended

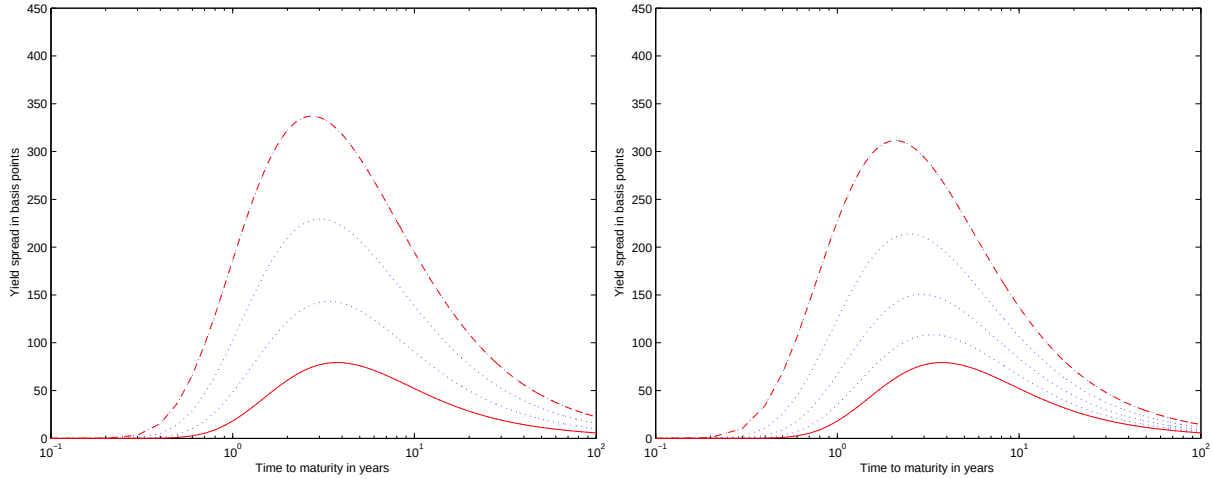

Figure 1: *The plots on the left show the sensitivity of the yield spread curve to the volatility level. The leverage of the firm B/x is set to $1/1.3$, the interest rate r is 6% and the curves increase with the values of σ: 10%, 11%, 12% and 13%. Note that the time to maturity is in unit of years and plotted on the log scale and the yield spread is quoted in basis points. The plots on the right show the sensitivity of the yield spread to the leverage level with the volatility level set to 10%. The curves increases with the increasing leverage ratios $B/x = (1/1.3, 1/1.275, 1/1.25, 1/1.225, 1/1.2)$.*

discussion, we refer to [9] and the references therein. In order to illustrate our approach we consider first the case where volatility is driven by one factor which we assume to be a mean-reverting Gaussian diffusion, i.e. an Ornstein-Uhlenbeck process. The dynamics under the physical measure $I\!P$ is described by the following pair of SDEs

$$dX_t = \mu X_t dt + f_1(Y_t) X_t \, dW_t^{(0)}, \tag{13}$$

$$dY_t = \alpha(m - Y_t)dt + \nu\sqrt{2\alpha}\, dW_t^{(1)}, \tag{14}$$

where we assume that

- The volatility function f_1 is positive, non-decreasing, and bounded above and away from zero.
- The invariant distribution of the volatility factor Y is the Gaussian distribution with mean m and standard deviation ν and it is independent of the parameter α.
- The important parameter $\alpha > 0$ is the *rate of mean reversion* of the process Y. In other words $1/\alpha$ is the *time scale* of this process, meaning that it reverts to its mean over times of order $1/\alpha$. Small values of α correspond to slow mean reversion and large values of α correspond to fast mean reversion.

- The standard Brownian motions $W^{(0)}$ and $W^{(1)}$ are correlated as

$$d\left\langle W^{(0)}, W^{(1)} \right\rangle_t = \rho_1 \, dt, \tag{15}$$

  where ρ_1 is a constant correlation coefficient, with $|\rho_1| < 1$.

We remark that for the purpose of illustration we choose the volatility factor to be an Ornstein-Uhlenbeck process. However, in our approach, Y could be any ergodic diffusion with a unique invariant distribution, as explained in more detail in [9]. Moreover, in our simulations we choose particular volatility functions $f_1(y)$ as being proportional to $\max(c_1, \min(c_2, \exp(y)))$, that is the exponential function with lower and upper cutoffs. In Section 5, we use the results of an asymptotic analysis of this model in the regime with Y being a slowly varying process corresponding to α being small. This requires that f_1 is smooth at the current level of the volatility factor y, which is the case here since cutoffs affect only the tails of f_1. In the illustration below, we choose $c_1 = 0.01$ and $c_2 = 5$. These particular choices of Y and f_1 are not essential for the perturbation method and the associated formulas presented in Section 4.

In order to price defaultable bonds under this model for the underlying, we rewrite it under a risk neutral measure $I\!P^\star$ chosen by the market through the market price of volatility risk Λ_1:

$$\begin{aligned} dX_t &= rX_t dt + f_1(Y_t) X_t \, dW_t^{(0)\star}, \\ dY_t &= \left(\alpha(m - Y_t) - \nu\sqrt{2\alpha}\Lambda_1(Y_t)\right) dt + \nu\sqrt{2\alpha} \, dW_t^{(1)\star}. \end{aligned} \tag{16}$$

Here $W^{(0)\star}$ and $W^{(1)\star}$ are standard Brownian motions under $I\!P^\star$ correlated as $W^{(0)}$ and $W^{(1)}$. We assume that the market price of volatility risk Λ_1 is bounded and a function of y only.

3.2 Stochastic Volatility Effects in Yield Spreads

In this section, we compute the yield spread that results when we use the *stochastic volatility* model in (16). Our focus is the combined role of the mean reversion time $1/\alpha$ and the correlation ρ_1 on the yield spread curve. We use various values for α, corresponding to volatility factors that range from slowly mean reverting ($\alpha = .05$) to fast mean reverting ($\alpha = 10$). For each value of α we present a slightly *negatively* correlated case ($\rho_1 = -0.05$). The effect of a stronger correlation, in addition to fast mean-reversion, is also shown in Figure 3 (bottom).

In each set of three plots, the top plot gives the yield spread curves as functions of time to maturity, and the starred curve corresponds to a constant volatility. The solid (higher) curve is the yield curve under the stochastic volatility model (16), where the initial volatility level $f_1(Y_0)$ and the long-run average volatility (see (18) below) coincide with the volatility level for the constant volatility case. The middle plot is analogous, but plotted on a log scale for the time to maturity to resolve the short maturity horizon behavior. The bottom plot shows one realization of the volatility process $f_1(Y)$ for the corresponding time scale parameters. The constant volatility yields are computed using the explicit formula (12). The stochastic volatility yields are computed using

Monte Carlo simulations of trajectories for the model (16). For these illustrations we choose the following parameter values: $\Lambda_1 = 0, x/B = 1.3, f_1(Y_0) = 0.12, r = 0.06, m = 0, \nu = 0.5$.

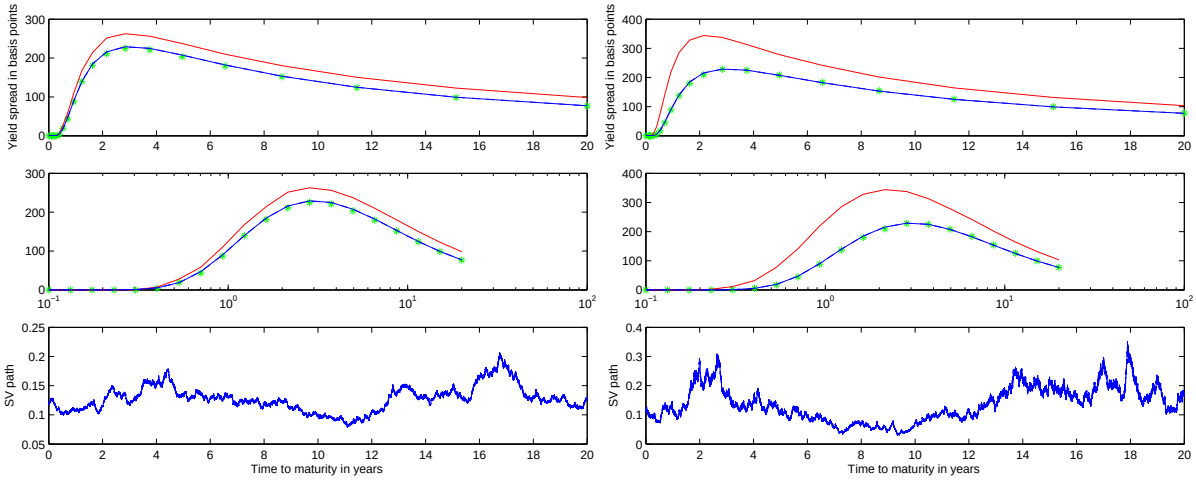

Figure 2: *Correlated ($\rho_1 = -0.05$) mean-reverting stochastic volatility: slowly ($\alpha = 0.05$) on the left, and order one ($\alpha = 0.5$) on the right.*

Figure 2 (left) illustrates the effects of a slowly mean reverting volatility with negative correlation. The yields for short maturities are not significantly affected. There is a mild spread increase for longer maturities. (This increase is slightly lower with zero correlation). This feature of the curve will be captured by analyzing the effect of a slow volatility factor in our model in Section 5.

Figure 2 (right) illustrates the effects of stochastic volatility that runs on the order one time scale. We observe that the effect is similar to an increase in volatility as shown in Figure 1. (This effect is enhanced by negative correlation over the zero correlation case, which is not shown here). This feature of the curve will be captured in the leading order term by choosing an appropriate effective volatility level $\sigma^\star$ in Section 4.3.

Finally, Figure 3 illustrates the effects of a fast mean reverting volatility, with negative correlation. In this case, the yields for short maturities are significantly affected with a small negative correlation (top row, for different leverage ratios) and even more so with a stronger correlation (bottom graph). It is remarkable that this effect is qualitatively and quantitatively very different from the effect resulting from an increase in the volatility level as shown in Figure 1. This feature of the curve will be captured in our analysis of the stochastic volatility model with a fast mean reverting volatility factor in the following section.

We conclude from these numerical experiments that the time scale content of stochastic volatility is crucial in the shaping of the yield spread curve. In particular, a short time scale combined with a negative correlation gives enhanced spreads at short maturities, as compared with the constant volatility case.

In Figure 3 (top right), we illustrate the effect of correlated fast mean reverting volatility in the case of a higher levered bond ($x/B = 1.2$). We observe that the spread at short maturities are significantly higher and again that this effect is qualitatively and quantitatively different from the effect seen by simply decreasing the level of x/B as seen in Figure 1.

A well separated fast volatility time scale has been observed in equity [10] and fixed income [6] markets. A main feature of this short time scale is that it can be treated by singular perturbation techniques as described in detail in [9]. This leads to a description where the effects of the stochastic volatility can be summarized in terms of two group market parameters, an effective constant volatility $\sigma^\star$ and a skew parameter R_3 (which are defined below). Here, we generalize these results to the case of defaultable bonds and show how these parameters can be conveniently calibrated from the observed yield spread curves. In Section 5, we also introduce a slow volatility time scale, which helps in modeling the yield spread curve at longer maturities.

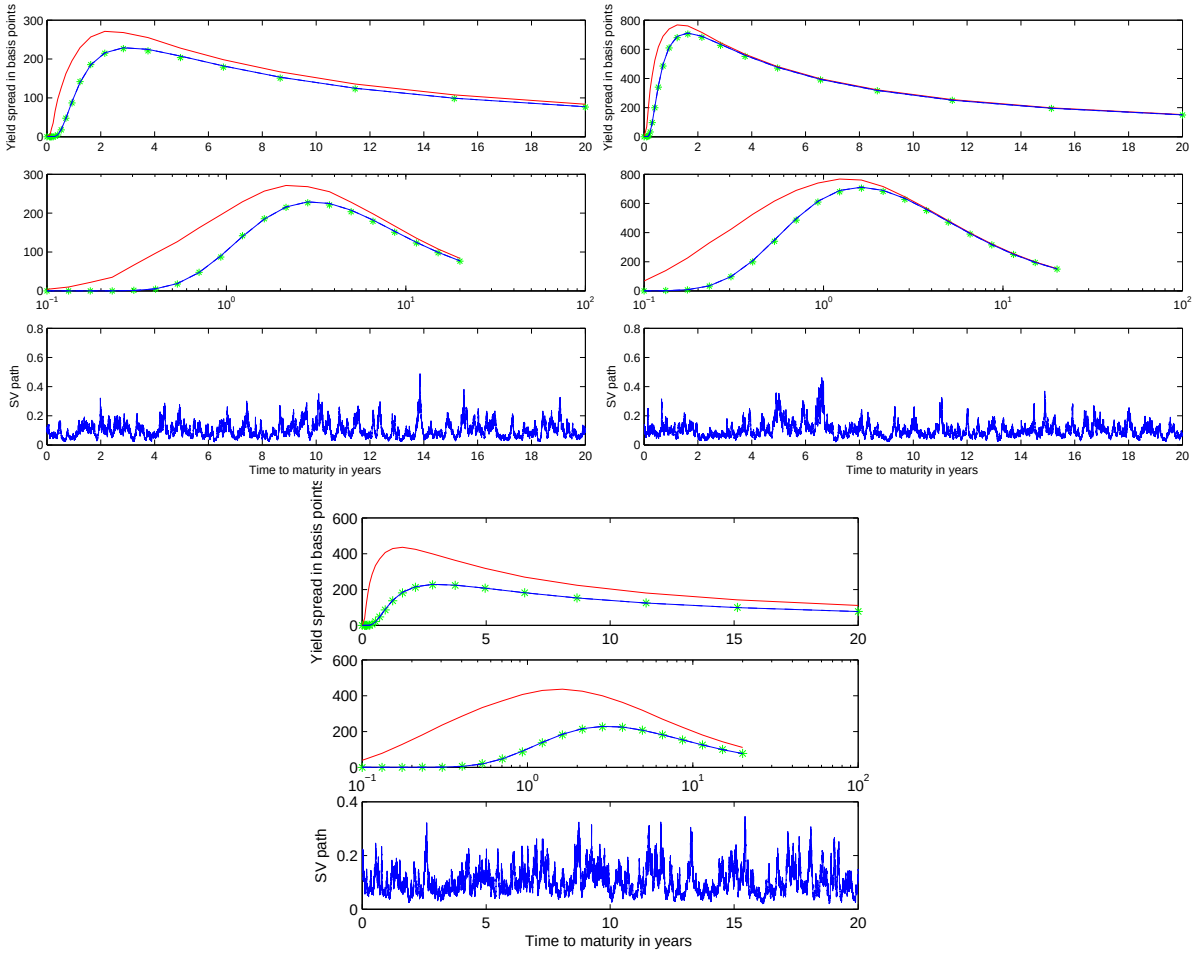

Figure 3: *Fast mean-reverting ($\alpha = 10$) stochastic volatility : moderately correlated ($\rho_1 = -0.05$) and moderately leveraged $B/x = 1/1.3$ (top left); moderately correlated ($\rho_1 = -0.05$) and more highly leveraged $B/x = 1/1.2$ (top right); and more strongly correlated ($\rho_1 = -0.5$) and moderately leveraged $B/x = 1/1.3$ (bottom).*

4 Fast Volatility Factor and Singular Perturbation

In this section, we analyze the effects of a fast mean-reverting volatility factor on defaultable bond prices. Mathematically this involves singular perturbation analysis of barrier options under stochastic volatility models (16), in the limit $\alpha \to \infty$.

4.1 The European Case

We recall first the singular perturbation results in the case of a European option. Let the payoff function at the maturity time T be $h(x)$. We denote by $P_{BS}(t,x;\sigma)$ the Black-Scholes price of this contract at time t when the stock price is x and the constant volatility is σ.

The price of the option in the stochastic volatility model (16) is obtained as the expected value of the discounted payoff under the risk neutral measure :

$$P(t,x,y) \;=\; I\!E^{\star}\left\{e^{-r(T-t)}h(X_T) \mid X_t = x, Y_t = y\right\}. \tag{17}$$

In [9] it is shown that in the limit of the volatility time scale going to zero, that is, $\alpha \to \infty$, the price P converges to the Black-Scholes price computed with an *effective* constant volatility $\bar{\sigma}$ given by

$$\bar{\sigma}^2 \;=\; \left\langle f_1^2 \right\rangle \;:=\; \int f_1^2(y)\Phi(y)\,dy, \tag{18}$$

where f_1^2 is averaged with respect to the invariant distribution of the Ornstein-Uhlenbeck process

$$\Phi(y) = \frac{1}{\sqrt{2\pi\nu^2}}\, e^{-(y-m)^2/2\nu^2}.$$

This limiting price is $P_{BS}(t,x;\bar{\sigma})$, which satisfies the following problem

$$\mathcal{L}_{BS}(\bar{\sigma})P_{BS} = 0\,, \tag{19}$$

$$P_{BS}(T,x) = h(x), \tag{20}$$

where $\mathcal{L}_{BS}(\bar{\sigma})$ is the Black-Scholes operator (5) at the volatility level $\bar{\sigma}$.

The main effects of stochastic volatility are captured by the first order correction proportional to $1/\sqrt{\alpha}$ and denoted by $P_1(t,x)$. It is given as the solution of the problem

$$\mathcal{L}_{BS}(\bar{\sigma})P_1 = -R_2 x^2 \frac{\partial^2 P_{BS}}{\partial x^2} - R_3 x \frac{\partial}{\partial x}\left(x^2 \frac{\partial^2 P_{BS}}{\partial x^2}\right),$$

$$P_1(T,x) = 0\,,$$

where P_{BS} is evaluated at $(t,x,\bar{\sigma})$. The parameters R_2 and R_3 are small of order $\sqrt{1/\alpha}$, and are complicated functions of the original model parameters:

$$R_2 = \frac{\nu}{\sqrt{2\alpha}}\langle \Lambda_1 \phi' \rangle, \qquad R_3 = -\frac{\rho_1 \nu}{\sqrt{2\alpha}}\langle f_1 \phi' \rangle, \tag{21}$$

where

$$\phi'(y) = \frac{1}{\nu^2 \Phi} \int_{-\infty}^{y} \left(f_1(u)^2 - \bar{\sigma}^2 \right) \Phi(u)\, du.$$

These formulas relating R_2, R_3 to the original model parameters will not be used explicitly in practice. In fact we explain in Section 7 how to calibrate directly these parameters from observed yield spreads. In terms of the notation (V_2, V_3) used in [9], the more convenient notation used here is related via $R_2 = 2V_3 - V_2$ and $R_3 = -V_3$.

Note that the first order price approximation

$$P(t, x, y) \approx P_{BS}(t, x; \bar{\sigma}) + P_1(t, x)$$

does not depend on the current level y of the volatility factor which is not directly observed.

The calibration is simplified by employing the following alternative approximation, which has the same order of accuracy. Introducing the corrected effective volatility $\sigma^\star$ by

$$\sigma^{\star 2} \quad = \quad \bar{\sigma}^2 + 2R_2, \tag{22}$$

the first term in the new approximation is $P_{BS}(t, x; \sigma^\star)$. This leads to the correction $P_1^\star$ being defined by

$$\begin{aligned} &\mathcal{L}_{BS}(\sigma^\star) P_1^\star = -R_3 x \frac{\partial}{\partial x} \left(x^2 \frac{\partial^2 P_{BS}}{\partial x^2}(t, x; \sigma^\star) \right), \\ &P_1^\star(T, x) = 0\,, \end{aligned} \tag{23}$$

so that

$$P(t, x, y) \approx P_{BS}(t, x; \sigma^\star) + P_1^\star(t, x). \tag{24}$$

The accuracy of this approximation is of order $1/\alpha$ in the case of a smooth payoff h, and of order $\log(\alpha)/\alpha$ in the case of call options as proved in [11].

Observe that $\sigma^\star$ and R_3 are the only parameters needed to compute this approximation, in fact, they can be calibrated from implied volatilities as explained in [13]. In Section 7, we generalize this calibration procedure to the case of defaultable bonds.

4.2 Barrier Options

In Section 1.1, we recalled that the price of the defaultable bond is the price of a down and out barrier digital option. In this section we therefore present the perturbation techniques in the context of down and out barrier options. See also [18] for fast scale volatility asymptotics for boundary value problems arising from exotic options.

Here we consider an option that pays $h(X_T)$ at maturity time T if the the underlying stays above a level B before time T and zero otherwise. Under the model (16) for the underlying, the price at time zero of this down and out barrier option is given by

$$e^{-rT}I\!E^\star\left\{h(X_T)\mathbf{1}_{\{\inf_{0\le s\le T}X_s>B\}}\right\}.$$

We define $u(t,x,y)$ by

$$u(t,x,y) \;=\; e^{-r(T-t)}I\!E^\star\left\{h(X_T)\mathbf{1}_{\{\inf_{t\le s\le T}X_s>B\}} \mid X_t=x, Y_t=y\right\},$$

so that the price of the barrier option at time t is given by

$$\mathbf{1}_{\{\inf_{0\le s\le t}X_s>B\}}u(t,X_t,Y_t).$$

The function $u(t,x,y)$ satisfies for $x\ge B$ the problem

$$\begin{array}{ll}\left(\frac{\partial}{\partial t}+\mathcal{L}_{X,Y}-r\right)u=0 & \text{on } x>B,\, t<T,\\ u(t,B,y)=0 & \text{for } t\le T,\\ u(T,x,y)=h(x) & \text{for } x>B,\end{array}$$

where $\mathcal{L}_{X,Y}$ is the infinitestimal generator of the process (X,Y) given by (16).

As in the European case, for calibration purposes, it is convenient to construct an asymptotic approximation in terms of the corrected effective volatility $\sigma^\star$ defined in (22). Hence, we define $u_0^\star(t,x)$ as the solution of the problem

$$\begin{array}{ll}\mathcal{L}_{BS}(\sigma^\star)u_0^\star=0 & \text{on } x>B,\, t<T,\\ u_0^\star(t,B)=0 & \text{for } t\le T,\\ u_0^\star(T,x)=h(x) & \text{for } x>B,\end{array} \tag{25}$$

and we find the correction $u_1^\star(t,x)$ solves

$$\begin{array}{ll}\mathcal{L}_{BS}(\sigma^\star)u_1^\star=-R_3\,x\frac{\partial}{\partial x}\left(x^2\frac{\partial^2u_0^\star}{\partial x^2}\right) & \text{on } x>B,\, t<T,\\ u_1^\star(t,B)=0 & \text{for } t\le T,\\ u_1^\star(T,x)=0 & \text{for } x>B.\end{array}$$

The derivation follows as in the derivation of (23), with the additional knock-out boundary condition at $x=B$. Remarkably, the small parameter R_3 is the same as in the European case.

For computing $u_1^\star$, it is convenient to replace the source problem above by a homogeneous problem with a non-homogeneous boundary condition. This is achieved by introducing $v_1^\star$ defined as

$$v_1^\star(t,x)=u_1^\star(t,x)-(T-t)R_3\,x\frac{\partial}{\partial x}\left(x^2\frac{\partial^2u_0^\star}{\partial x^2}(t,x)\right),$$

so that $v_1^\star(t,x)$ solves the simpler problem

$$\begin{array}{ll} \mathcal{L}_{BS}(\sigma^\star)v_1^\star = 0 & \text{on } x > B,\, t < T, \\ v_1^\star(t,B) = g(t) & \text{for } t \le T, \\ v_1^\star(T,x) = 0 & \text{for } x > B, \end{array} \tag{26}$$

with the function $g(t)$ given by

$$g(t) = -R_3\,(T-t)\lim_{x\downarrow B} F_3(t,x),$$

where we define

$$F_3(t,x) \;=\; x\frac{\partial}{\partial x}\left(x^2\frac{\partial^2 u_0^\star}{\partial x^2}(t,x)\right). \tag{27}$$

To summarize, we have

$$u(t,x,y) \;\approx\; u_0^\star(t,x) + (T-t)R_3\,F_3(t,x) + v_1^\star(t,x) \tag{28}$$

where $u_0^\star$ and $v_1^\star$ are given in (25) and (26) respectively.

4.3 Pricing Defaultable Bonds

In this section, we consider the case $h(x) = 1$ corresponding to a defaultable zero coupon bond. In this case, $u_0^\star$ defined in (25) is explicitly given by

$$u_0^\star(t,x) = u_{BS}(t,x;\sigma^\star), \tag{29}$$

where u_{BS} was defined in (8)-(9).

Calculations for the $h = 1$ case given in Appendix A lead to the formula

$$g(t) \;=\; R_3 e^{-r(T-t)}\left[\frac{1}{\sigma^{\star 3}}\left(\frac{2}{\sqrt{T-t}} + 4pr\sqrt{T-t}\right)N'(d) + (T-t)(p-1)p^2N(d)\right] \tag{30}$$

$$d \;=\; -\frac{p\sigma^\star\sqrt{T-t}}{2}, \tag{31}$$

where

$$p = 1 - \frac{2r}{\sigma^{\star 2}},$$

and the formula for F_3 defined in (27) is given in equation (56) there.

The problem (26) for $v_1^\star$ admits the probabilistic representation

$$v_1^\star(t,x) = I\!E^\star\{e^{-r(\xi-t)}g(\xi)\mathbf{1}_{\{\xi\le T\}} \mid X_t^\star = x > B\} \tag{32}$$

where $X^\star$ is a geometric Brownian motion with volatility $\sigma^\star$ and ξ is the first time $X^\star$ hits the boundary B.

By changing to log coordinates and using a Girsanov transformation, the problem is rewritten as a first passage problem for a driftless Brownian motion. The distribution of the first hitting time is known (see for instance [19, Chapter 2]) and v_1 can then be written as a Gaussian integral. We obtain

$$v_1^\star(t,x) \;=\; \frac{\left(\frac{x}{B}\right)^{\frac{p}{2}}}{\sigma^\star\sqrt{2\pi}}\int_t^T \frac{\log(x/B)}{(s-t)^{3/2}} e^{-\frac{(\log(x/B))^2}{2\sigma^{\star 2}(s-t)}} e^{-\left(r+(\sigma^\star p)^2/8\right)(s-t)} g(s)\,ds, \tag{33}$$

where the function g, which is proportional to the small parameter R_3, is given in (30).

Therefore, the price $\Gamma^B(0,T)$ of the defaultable bond at time zero, defined in (1), is approximated by

$$\Gamma^B(0,T) \;\approx\; u_0^\star(0,x) + TR_3\,F_3(0,x) + v_1^\star(0,x) \tag{34}$$

where $u_0^\star(t,x)$, $F_3(t,x)$, and $v_1^\star(t,x)$ are given in (29), (56), and (33) respectively.

In Figure 4, the yield corresponding to this price approximation is represented by the dashed line, and the yield corresponding to the constant volatility price $u_0^\star(t,x)$ is represented by the solid line. We use the following values of the parameters $\sigma^\star = 0.12, r = 0, R_3 = -0.0003, x/B = 1.2$ and present the top plot on a linear scale and the bottom in log maturity coordinates. One sees that the correction has qualitatively the shape of the correction seen in Figure 3 (right). The stochastic volatility strongly affects the yields for short maturities and the effect is very different from that obtained if only the volatility level is changed. Accuracy of the asymptotic approximation, with respect to a given, fully specified stochastic volatility model, will be discussed in Section 6.3.

5 Slow Volatility Factor and Regular Perturbation

We have seen in the previous section that the correction generated by the fast mean-reverting stochastic volatility factor affects the yield spreads mainly at short maturities. To gain more flexibility in calibrating yield spreads we introduce a slow volatility factor which will help the fit at longer maturities. The importance of this is demonstrated in the calibration in Section 7. In this section, we summarize the correction generated by a *slow* volatility factor corresponding to α small in (16). We denote this factor by Z and its time scale parameter by δ to distinguish from the fast case analyzed previously. We will combine both fast and slow factors in Section 6.

We rewrite the dynamics of the underlying under the risk neutral measure $I\!P^\star$ as

$$\begin{aligned} dX_t &= rX_t\,dt + f_2(Z_t)X_t\,dW_t^{(0)\star}, \\ dZ_t &= \left(\delta(m_2 - Z_t) - \nu_2\sqrt{2\delta}\Lambda_2(Z_t)\right)dt + \nu_2\sqrt{2\delta}\,dW_t^{(2)\star}, \end{aligned} \tag{35}$$

where we assume that

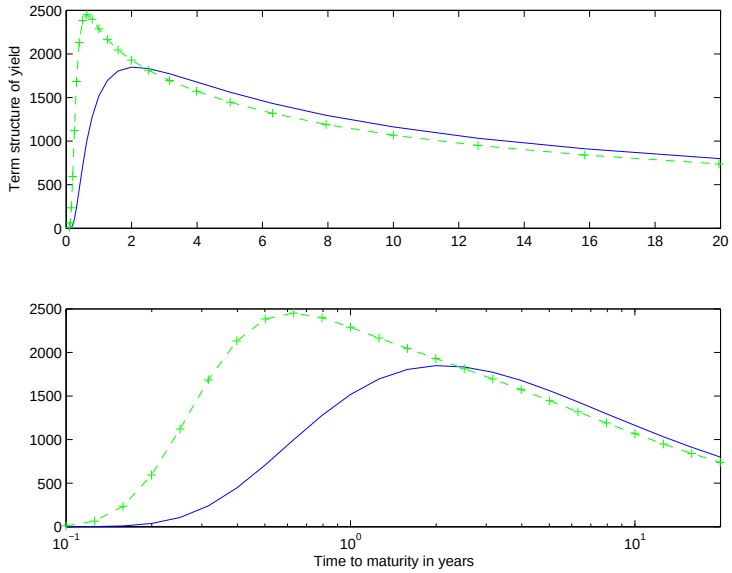

Figure 4: *The approximated yield for* $\sigma^\star = 0.12, r = 0.0, R_3 = -0.0003, x/B = 1.2$. *The solid line corresponds to the constant volatility leading order term. The crossed dashed line incorporates the stochastic volatility correction. The top plot is on the linear scale and the bottom plot is on the log maturity scale.*

- The volatility function f_2 is positive, smooth, non-decreasing, bounded above and away from zero.
- The function $\Lambda_2(z)$ is a market price of volatility risk.
- The small parameter $\delta > 0$ corresponds to the long time scale $1/\delta$, and the volatility factor Z_t changes slowly.
- The standard Brownian motions $W^{(0)}$ and $W^{(2)}$ are correlated as

$$d\left\langle W^{(0)}, W^{(2)} \right\rangle_t \quad = \quad \rho_2 \, dt, \tag{36}$$

  where ρ_2 is a constant correlation coefficient satisfying $|\rho_2| < 1$.

Following [12] and [13], the price of a derivative written on an underlying governed by (35) can be approximated by regular perturbation techniques in the regime δ small. The price of a defaultable bond is given by

$$\Gamma^B(t,T) = \mathbf{1}_{\{\inf_{0\le s\le t} X_s > B\}} u(t, X_t, Z_t),$$

where $u(t,x,z)$ satisfies the problem

$$\begin{array}{ll} \left(\frac{\partial}{\partial t}+\mathcal{L}_{X,Z}-r\right)u=0 & \text{on } x>B,\, t<T, \\ u(t,B,z)=0 & \text{for } \quad t\leq T, \\ u(T,x,z)=1 & \text{for } \quad x>B. \end{array}$$

Here, $\mathcal{L}_{X,Z}$ is the infinitestimal generator of the process (X,Z) given by (35).

The leading order term $u_0^{(z)}(t,x)$, in the expansion $u=u_0^{(z)}+u_1^{(z)}+\cdots$, solves the problem

$$\begin{array}{ll} \mathcal{L}_{BS}(f_2(z))u_0^{(z)}=0 & \text{on } x>B,\, t<T, \\ u_0^{(z)}(t,B)=0 & \text{for } \quad t\leq T, \\ u_0^{(z)}(T,x)=1 & \text{for } \quad x>B, \end{array} \tag{37}$$

where z is only a parameter which corresponds to the current "frozen" level of the slow volatility factor. The function $u_0^{(z)}(t,x)$ is given explicitly by

$$u_0^{(z)}(t,x)=u_{BS}(t,x;f_2(z)),$$

where u_{BS} was defined in (8)-(9).

The first correction $u_1^{(z)}(t,x)$ solves the problem

$$\begin{array}{ll} \mathcal{L}_{BS}(f_2(z))u_1^{(z)}=-2\left(R_0(z)\frac{\partial u_{BS}}{\partial\sigma}+R_1(z)x\frac{\partial}{\partial x}\left(\frac{\partial u_{BS}}{\partial\sigma}\right)\right) & \text{on } x>B,\, t<T, \\ u_1^{(z)}(t,B)=0 & \text{for } \quad t\leq T, \\ u_1^{(z)}(T,x)=0 & \text{for } \quad x>B, \end{array} \tag{38}$$

where u_{BS} is evaluated at $(t,x,f_2(z))$, and $R_0(z)$ and $R_1(z)$ are small parameters of order $\sqrt{\delta}$, functions of the model parameters:

$$\begin{aligned} R_0(z) &= -\sqrt{\frac{\delta}{2}}\,\nu_2\Lambda_2(z)f_2'(z) \\ R_1(z) &= \sqrt{\frac{\delta}{2}}\,\rho_2\nu_2 f_2(z)f_2'(z), \end{aligned}$$

and depending on the current level z of the slow factor.

We again transform this source problem into a homogeneous problem with a non-homogeneous boundary condition. This is done in three steps. We first introduce

$$u_{1a}^{(z)}(t,x) = 2(T-t)\left(R_0(z)\frac{\partial u_{BS}}{\partial\sigma}+R_1(z)x\frac{\partial}{\partial x}\left(\frac{\partial u_{BS}}{\partial\sigma}\right)\right), \tag{39}$$

and then we define

$$u_{1b}^{(z)}(t,x) \quad = \quad u_1^{(z)}(t,x) - u_{1a}^{(z)}(t,x). \tag{40}$$

Using the relations

$$\mathcal{L}_{BS}(f_2(z))\left(\frac{\partial u_{BS}}{\partial \sigma}\right) = -f_2(z)x^2\frac{\partial^2 u_{BS}}{\partial x^2},$$
$$\mathcal{L}_{BS}(f_2(z))\left(x\frac{\partial}{\partial x}\left(\frac{\partial u_{BS}}{\partial \sigma}\right)\right) = -f_2(z)x\frac{\partial}{\partial x}\left(x^2\frac{\partial^2 u_{BS}}{\partial x^2}\right),$$

we obtain that $u_{1b}^{(z)}$ solves

$$\begin{array}{ll} \mathcal{L}_{BS}(f_2(z))u_{1b}^{(z)} = 2(T-t)f_2(z)\left(R_0(z)x^2\frac{\partial^2 u_{BS}}{\partial x^2} + R_1(z)x\frac{\partial}{\partial x}\left(x^2\frac{\partial^2 u_{BS}}{\partial x^2}\right)\right) & \text{on } x > B,\, t < T, \\ u_{1b}^{(z)}(t,B) = g_b(t) & \text{for } t \le T, \\ u_{1b}^{(z)}(T,x) = 0 & \text{for } x > B, \end{array} \tag{41}$$

with

$$g_b(t) = \lim_{x\downarrow B}\left(u_1^{(z)}(t,x) - u_{1a}^{(z)}(t,x)\right) = -\lim_{x\downarrow B} u_{1a}^{(z)}(t,x), \tag{42}$$

since $u_1^{(z)}(t,B) = 0$. Notice that the source term in (41) is now in terms of x-derivatives of u_{BS}. We are now able to remove the source in (41) by introducing

$$u_{1c}^{(z)}(t,x) \quad = \quad -(T-t)^2 f_2(z)\left(R_0(z)x^2\frac{\partial^2 u_{BS}}{\partial x^2} + R_1(z)x\frac{\partial}{\partial x}\left(x^2\frac{\partial^2 u_{BS}}{\partial x^2}\right)\right), \tag{43}$$

and defining

$$u_{1d}^{(z)}(t,x) \quad = \quad u_{1b}^{(z)}(t,x) - u_{1c}^{(z)}(t,x), \tag{44}$$

which solves

$$\begin{array}{ll} \mathcal{L}_{BS}(f_2(z))u_{1d}^{(z)} = 0 & \text{on } x > B,\, t < T, \\ u_{1d}^{(z)}(t,B) = g_d(t) & \text{for } t \le T, \\ u_{1d}^{(z)}(T,x) = 0 & \text{for } x > B, \end{array} \tag{45}$$

with

$$g_d(t) \quad = \quad g_b(t) - \lim_{x\downarrow B} u_{1c}^{(z)}. \tag{46}$$

To summarize, we have

$$u(t,x,z) \quad \approx \quad u_{BS}(t,x;f_2(z)) + u_{1a}^{(z)}(t,x) + u_{1c}^{(z)}(t,x) + u_{1d}^{(z)}(t,x), \tag{47}$$

where $u_{1a}^{(z)}$ is given by (39), $u_{1c}^{(z)}$ is given by (43), and $u_{1d}^{(z)}$ solves (45).

Equation (45) for $u_{1d}^{(z)}$, the last contribution to the approximation (47), can be solved by rewriting it in the log-variable $\log x$, and using distributions for the hitting times of Brownian motions as in Section 4.3. We obtain

$$u_{1d}^{(z)}(t,x) = \frac{\left(\frac{x}{B}\right)^{\frac{p}{2}}}{f_2(z)\sqrt{2\pi}} \int_t^T \frac{\log(x/B)}{(s-t)^{3/2}} \exp\left(-\frac{(\log(x/B))^2}{2f_2(z)^2(s-t)} - \left[\frac{(f_2(z)p)^2}{8} + r \right] (s-t) \right) g_d(s)\, ds, \tag{48}$$

where $g_d(t)$ is defined in (46), and we have the formula (60) given in Appendix B.

In Figure 5 the yield corresponding to the price approximation (47) is represented by the dashed line, and the yield corresponding to the constant volatility price $u_{BS}(t,x;f_2(z))$ is represented by the solid line. We use the following values of the parameters $f_2(z) = 0.12, r = 0.0, R_0(z) = 0.0003, R_1(z) = -0.0005, x/B = 1.2$ and present the top plot on a linear scale and the bottom in log coordinates. One sees that the correction has qualitatively the shape of the correction seen in Figure 2. The stochastic volatility affects the yields for longer maturities with small effects on short maturities. Accuracy of the asymptotic approximation, with respect to a given, fully specified stochastic volatility model, will be discussed in Section 6.3.

6 Models with Fast & Slow Volatility Factors

In this section we consider a class of models which include two stochastic volatility factors with separated time scales, one fast and the other one slow. We then combine singular and regular perturbations to obtain an approximation for the defaultable bond price. Finally we discuss the calibration of the parameters needed in this approximation.

6.1 The Combined Two Scale Stochastic Volatility Models

Under the risk-neutral pricing measure $\mathbb{P}^\star$, our model is a combination of (16) and (35) as follows:

$$\begin{aligned} dX_t &= rX_t dt + f(Y_t,Z_t)X_t\, dW_t^{(0)\star}, \\ dY_t &= \left(\frac{1}{\varepsilon}(m_1 - Y_t) - \frac{\nu_1\sqrt{2}}{\sqrt{\varepsilon}} \Lambda_1(Y_t,Z_t) \right) dt + \frac{\nu_1\sqrt{2}}{\sqrt{\varepsilon}}\, dW_t^{(1)\star}, \\ dZ_t &= \left(\delta(m_2 - Z_t) - \nu_2\sqrt{2\delta}\, \Lambda_2(Y_t,Z_t) \right) dt + \nu_2\sqrt{2\delta}\, dW_t^{(2)\star}, \end{aligned} \tag{49}$$

where we assume that

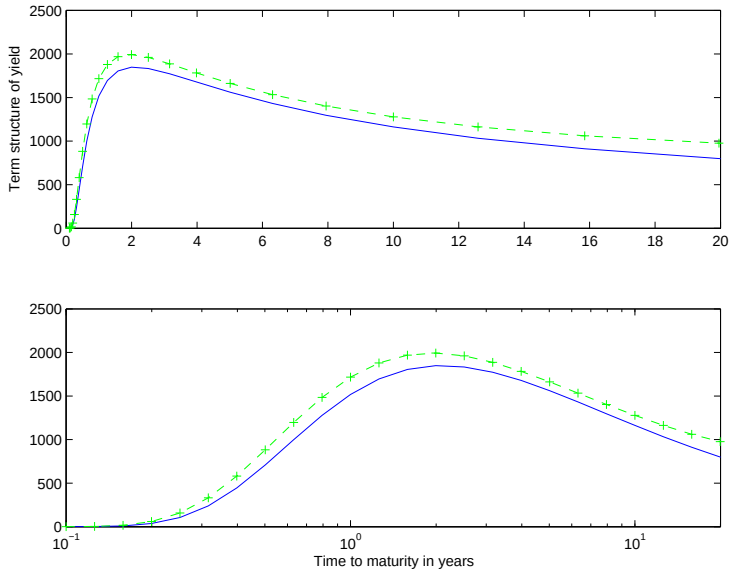

Figure 5: *The approximated yield for* $f_2(z) = 0.12, r = 0.0, R_0(z) = 0.0003, R_1(z) = -0.0005, x/B = 1.2$. *The solid line corresponds to the constant volatility leading order term. The dashed line incorporates the slow varying stochastic volatility correction. The bottom plot is in the log scale and the top plot is in the original scale.*

- The volatility function $f(y, z)$ is positive, smooth in z, non-decreasing, bounded above and away from zero.
- The functions $\Lambda_1(y, z)$ and $\Lambda_2(y, z)$ are the combined market prices of volatility risk which determine $I\!P^\star$ chosen by the market.
- The short time scale ε and the long time scale $1/\delta$ are such that

$$\varepsilon << 1 << \frac{1}{\delta}.$$

- The standard Brownian motions $\left(W_t^{(0)\star}, W_t^{(1)\star}, W_t^{(2)\star}\right)$ are correlated according to the following cross-variations:

$$\begin{aligned} d\langle W^{(0)\star}, W^{(1)\star}\rangle_t &= \rho_1 dt, \\ d\langle W^{(0)\star}, W^{(2)\star}\rangle_t &= \rho_2 dt, \\ d\langle W^{(1)\star}, W^{(2)\star}\rangle_t &= \rho_{12} dt, \end{aligned}$$

  where $|\rho_1| < 1$, $|\rho_2| < 1$ and $|\rho_{12}| < 1$.

- The unperturbed volatility process Y_t, that is without Λ_1, admits the Gaussian invariant distribution $\mathcal{N}(m_1, \nu_1^2)$. Averaging with respect to this invariant distribution is again denoted by $\langle\cdot\rangle$.

Under this model, the price at time $t < T$ of a zero-coupon defaultable bond maturing at T is given by

$$\Gamma^B(t,T) = \mathbf{1}_{\{\inf_{0\le s\le t} X_s > B\}} u(t, X_t, Y_t, Z_t),$$

where $u(t,x,y,z)$ satisfies the problem

$$\begin{array}{ll} \left(\frac{\partial}{\partial t} + \mathcal{L}_{X,Y,Z} - r\right) u = 0 & \text{on } x > B,\ t < T, \\ u(t,B,y,z) = 0 & \text{for } t \le T, \\ u(T,x,y,z) = 1 & \text{for } x > B, \end{array}$$

and $\mathcal{L}_{X,Y,Z}$ is the infinitesimal generator of the process (X,Y,Z) given by (49). The function $u(t,x,y,z)$ is approximated in the following section.

6.2 The Combined Volatility Perturbations

Following [12] and [13], one can combine the singular perturbation presented in Section 4, and the regular perturbation presented in Section 5, to obtain:

$$u(t,x,y,z) \;=\; u_0^{(z)}(t,x) + u_{1,\varepsilon}^{(z)}(t,x) + u_{1,\delta}^{(z)}(t,x) + \cdots,$$

where $u_0^{(z)}(t,x)$ is the order one leading term, $u_{1,\varepsilon}^{(z)}(t,x)$ is proportional to $\sqrt{\varepsilon}$, $u_{1,\delta}^{(z)}(t,x)$ is proportional to $\sqrt{\delta}$, and the following terms are of higher order in $\sqrt{\varepsilon}$ and $\sqrt{\delta}$. The method consists of expanding first in δ (regular perturbation) and then in ε (singular perturbation), although the reverse order leads to the same approximation. The singular perturbation analysis leads to effective group parameters $(\sigma^\star, R_3)$ as in Section 4, but these now depend on the "frozen" slow volatility factor level z. We obtain group parameters (R_0, R_1) from the regular perturbation expansion as in Section 5, and these also depend on z.

The function $u_0^{(z)}(t,x)$ is given by (29) where $\sigma^\star$ is now z-dependent and denoted by $\sigma^\star(z)$. The function $u_{1,\varepsilon}^{(z)}(t,x)$ is given by

$$u_{1,\varepsilon}^{(z)}(t,x) \;=\; (T-t) R_3(z)\, F_3^{(z)}(t,x) + v_1^{\star(z)}(t,x),$$

where $R_3(z)$ is a z-dependent parameter that is small of order $\sqrt{\varepsilon}$, and $F_3^{(z)}(t,x)$ and $v_1^{\star(z)}(t,x)$ are given by (56) in Appendix B and (33) respectively, with $\sigma^\star$ replaced by $\sigma^\star(z)$.

As in Section 5, the function $u_{1,\delta}^{(z)}(t,x)$ is the sum of three components

$$u_{1,\delta}^{(z)}(t,x) \;=\; u_{1a}^{(z)}(t,x) + u_{1c}^{(z)}(t,x) + u_{1d}^{(z)}(t,x),$$

given respectively by (39), (43) and (48) with $f_2(z)$ replaced by $\sigma^\star(z)$. In particular, the two parameters R_0 and R_1 involved in these components are small of order $\sqrt{\delta}$ and z-dependent.

In terms of the yield spreads $Y(0,T)$, generated by the full stochastic volatility model (49), we obtain the following approximation

$$\begin{aligned} r + Y(0,T) &= -\frac{1}{T}\log(u(0,x,y,z)) \\ &\approx -\frac{1}{T}\log\left(u_0^{(z)}(0,x) + u_{1,\varepsilon}^{(z)}(0,x) + u_{1,\delta}^{(z)}(0,x)\right) \\ &\approx -\frac{1}{T}\log\left(u_0^{(z)}(0,x)\right) - \frac{1}{T}\left(\frac{u_{1,\varepsilon}^{(z)}(0,x)}{u_0^{(z)}(0,x)}\right) - \frac{1}{T}\left(\frac{u_{1,\delta}^{(z)}(0,x)}{u_0^{(z)}(0,x)}\right), \end{aligned} \tag{50}$$

where

- The first term is the yield spread produced by the constant volatility model discussed in Section 2, evaluated at the volatility level $\sigma^\star(z)$. Therefore $\sigma^\star(z)$ is the parameter which controls the yield curve for intermediate maturities (say one to ten years).
- The second term is the correction scaled by the small parameter R_3 which affects primarily the short maturities as shown in Figure 3 (right).
- The third term is the correction scaled by the small parameters R_0 and R_1 which affect the longer maturities as shown in Figure 2.

In Figure 6 we show the yield corresponding to the price approximation corresponding to (50) that includes the correction terms from both the fast and the slow scales by the dashed line, and the yield corresponding to the constant volatility price $u_0^\star(t,x)$ by the solid line. We use the same values for the parameters as above $\sigma^\star = 0.12, r = 0.0, R_0 = 0.0003, R_1 = -0.0005, R_3 = -0.0003, x/B = 1.2$. The multiscale stochastic volatility affects the yields significantly for all maturities.

We discuss the error of the approximation (50) in the next section, and in Section 7, we analyze the form of the correction terms in more detail. In particular we examine how they depend on the group market parameters $(\sigma^\star, R_0, R_1, R_3)$, that is the parameters we estimate in the calibration step.

6.3 Accuracy of the Approximation

We first demonstrate the accuracy of the asymptotic approximation (in the fast mean-reverting case) with a numerical example, and then provide a precise analytical result for the rate of convergence of the complete two-factor (fast and slow) stochastic volatility model.

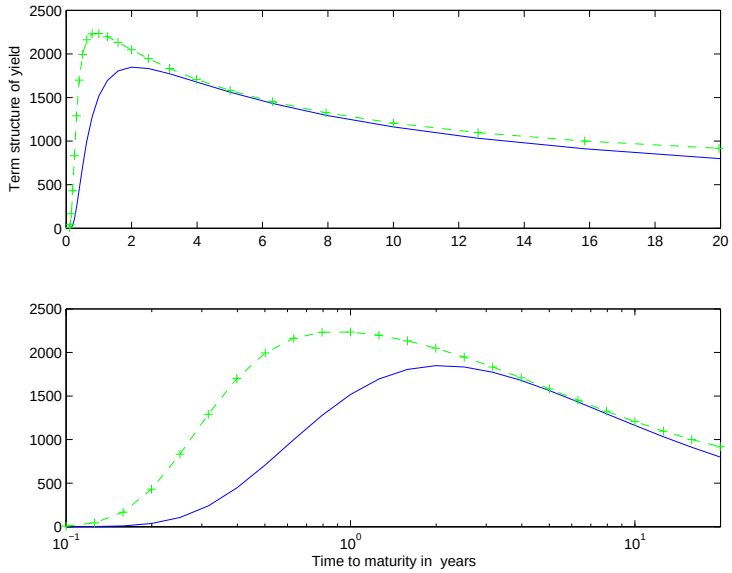

Figure 6: *The approximated yield for* $\sigma^\star = 0.12, r = 0.0, R_0 = 0.0003, R_1 = -0.0005, R_3 = -0.0003, x/B = 1.2$. *The solid line corresponds to the constant volatility leading order term. The dashed line incorporates the slow and fast varying stochastic volatility corrections. The bottom plot is in the log scale and the top plot is in the original scale.*

6.3.1 Illustration from Numerical Simulations

We consider a fully-specified one-factor fast mean-reverting stochastic volatility model (16) with the following choices:

$$r = 0.06, \quad \bar{\sigma} = 0.12, \quad \nu = 0.5, \quad f_1(y) = \bar{\sigma} e^{-\nu^2} e^y, \quad m = 0,$$

and with the market price of volatility risk $\Lambda_1 \equiv 0$. The rate of mean-reversion α varies from 5 to 50, corresponding to mean-reversion times from about two months down to about a week.

We compute by Monte Carlo simulations the yield spread (for each α) on a five-year defaultable bond with leverage $B/x = 1/1.3$. The starting values are $X_0 = 1, Y_0 = 0$. We compare with the approximation given by formula (34), converted to yield spread. The parameters needed in the approximation $(\sigma^\star, R_3)$ are related to the original model by formulas (18,21,22) and here are computed as $\bar{\sigma} = 0.12$, $R_3 = -7 \times 10^{-5}/\sqrt{\alpha}$ and $\sigma^\star = \bar{\sigma}$ since $R_2 = 0$ with our choice $\Lambda_1 \equiv 0$. For reference, the corresponding Black-Cox yield, with constant volatility $\bar{\sigma}$, is equal to 2.069%.

The following table shows the absolute relative pricing error between the asymptotic approximation and the true price computed with Monte Carlo (using a cautious 100,000 paths and 25,000 time-steps per path). Clearly, the error is decreasing as the rate of mean-reversion increases, and the magnitudes are small.

α	Relative Pricing Error
5	9.60×10^{-4}
20	5.92×10^{-4}
25	5.20×10^{-4}
35	3.07×10^{-4}
40	2.52×10^{-4}
50	1.29×10^{-4}

6.3.2 Convergence Result

We briefly outline how the accuracy result, obtained for call options in the singular perturbation case [11], and generalized to combined singular and regular perturbations in [12], can be adapted to the present situation of defaultable bonds viewed as digital down-and-out barrier options.

The payoff of a European digital option is discontinuous, and therefore less regular than that of an European call option. In order to establish the rate of convergence of the singular perturbation approximation, we use the regularization discussed in [11] which consists in controlling the successive derivatives of the Black-Scholes price with the regularized payoff, in terms of a regularization parameter η. In the case of the call, the first derivative can be taken on the original payoff, while the remaining derivatives are taken on the smoothing kernel. In the case of the digital, all the derivatives have to hit the kernel, and therefore it produces an extra $\eta^{-1/2}$. Consequently, the problem of optimal bounding of the error terms $(\eta, \varepsilon \log|\eta|, \frac{\varepsilon^{3/2}}{\sqrt{\eta}})$, obtained in [11], is now to optimally bound $(\eta, \frac{\varepsilon \log|\eta|}{\sqrt{\eta}}, \frac{\varepsilon^{3/2}}{\eta})$. The first error term is not affected by the derivatives since it comes from the regularization of the original price. By substituting $\eta = \varepsilon^q$, we reduce the problem to the following maxmin problem

$$\max \min \left\{ q, 1 - \frac{q}{2}, \frac{3}{2} - q \right\},$$

which admits the solution $q = 2/3$.

The regular perturbation with respect to δ gives an order of accuracy $\mathcal{O}(\delta)$, and therefore, pointwise in (t, x, y, z), the combined order of accuracy is $\mathcal{O}(\varepsilon^{2/3} \log|\varepsilon| + \delta)$.

The accuracy of the approximation (50) is obtained by generalizing the case of a digital option to the case of a digital barrier option. The first step is to regularize the terminal payoff by replacing it by the Black-Scholes price of the barrier option, with a small time-to-maturity η. As in the proof of convergence in the European case, the argument consists in controlling the blow-up of the successive x-derivatives at maturity and at the barrier, but now of the Black-Scholes price of the contract. By the method of images, this is reduced to the analysis of the Black-Scholes digital option formula and its derivatives. Consequently, there is a discontinuity in the payoff at the corner $(t = T, x = B)$ as in the case of a European binary option. Therefore the order of accuracy in this case is as with the digital, namely $\mathcal{O}(\varepsilon^{2/3} \log|\varepsilon| + \delta)$.

7 Calibration

In this section, we discuss calibration of the asymptotic approximation obtained in the previous section from yield spread data. The parameters of interest are $(\sigma^\star, R_0, R_1, R_3)$. We first reformulate the approximation in terms of yield, and then illustrate the ability of the model to fit observed yield spread data.

7.1 Calibration Formulas

We rewrite the approximated yield (50) as

$$Y(0,T) \approx Y^\star(T;\sigma^\star) + Y^\varepsilon(T;\sigma^\star) + Y^\delta(T;\sigma^\star)\,, \tag{51}$$

where the leading yield term is given explicitly by

$$Y^\star(T,\sigma^\star) = -\frac{1}{T}\log\left(N(d_2^+) - \left(\frac{x}{B}\right)^p N(d_2^-)\right)\,, \tag{52}$$

with

$$p = 1 - \frac{2r}{\sigma^\star}\,, \qquad d_2^\pm = \frac{\pm\log(x/B) + p\sigma^{\star 2}T/2}{\sigma^\star\sqrt{T}},$$

where we do not show the z-dependence in $\sigma^\star$, or in the parameters (R_0, R_1, R_3) below. The main yield term component $Y^\star$ typically captures well the observed yield curves at intermediate maturities. This component is generated by a first passage model with constant volatility $\sigma^\star$ which is therefore the only parameter to be calibrated in this case, if we assumed that the leverage B/x is known.

In this paper we have shown that an extended first passage model with multiscale stochastic volatility gives more flexibility to capture the behavior of the yield curve at short and long maturities. Moreover, by using perturbation techniques we have derived explicit formulas for the corrections Y^ε and Y^δ to the yield spread.

The first correction Y^ε is given by

$$Y^\varepsilon(T;\sigma^\star) = -\frac{1}{T}\left(\frac{R_3\ TF_3 + v_1^\star}{u_0^\star}\right)\,, \tag{53}$$

where $u_0^\star$, F_3, and $v_1^\star$ are evaluated at the current time $t=0$, current asset value x and maturity T, and given respectively by (29), (56), and (33). Observe from (30) that $v_1^\star$ is also proportional to the small parameter R_3 which is fitted in order to capture the yield spread behavior at short maturities.

Using the expression (57) for $u_{1a}^{(z)} + u_{1c}^{(z)}$ given in Appendix B, with $f_2(z)$ replaced by $\sigma^\star(z)$, the second correction Y^δ is given by

$$Y^\delta(T;\sigma^\star) = -\frac{1}{T}\left(\frac{R_0\left\{2TF_0 - T^2\sigma^\star F_2\right\} + R_1\left\{2TF_1 - T^2\sigma^\star F_3\right\} + u_{1d}}{u_0^\star}\right)\,, \tag{54}$$

where $u_0^\star$, F_0, F_1, F_2, F_3, and u_{1d} are evaluated at $t = 0$, current asset value x and maturity T, and given respectively by (29), (58), (59), (55), (56), and (48). Observe from (60) that u_{1d} is also a sum of terms proportional to either R_0 or R_1 which are the two small parameters to be fitted in order to capture the yield spread behavior at longer maturities.

7.2 Calibration Exercise

We demonstrate the versatility of the stochastic volatility models through the approximation formulas above, by manually fitting them to some market data. The specific components of the model, namely the base Black-Cox model enhanced with fast and slow stochastic volatility factors, have natural effects on the yield spreads produced: the base volatility $\sigma^\star$ and the leverage B/x entering the Black-Cox formula set the basic level of the curve; the fast factor, whose effect is described through the parameter R_3, influences the slope of the short end of the curve; and the parameters R_0 and R_1 associated with the slow factor impact the level and slope respectively of the long end of the curve. Of course, the effects of each parameter are not entirely independent, but the physical interpretation of their roles makes it natural to employ a visual fitting as a starting point for an automated procedure. A thorough empirical study with an optimized fitting procedure is beyond the scope of the current paper.

We take yield spreads from market prices of corporate bonds for two firms, Ford on 9 December 2004, when it was rated BBB, and IBM, a firm rated A or higher, on 1 December 2004. The spreads are obtained from `bondpage.com`. For simplicity, we assume a constant interest rate $r = 0.025$ throughout.

We first fit the Black-Cox yield spread by varying the volatility $\bar{\sigma}$ and the leverage B/x. This is shown by the solid line in Figures 7 and 8. As expected and well-documented, the shape generated by this model doesn't capture the data well, especially at shorter maturities. We next exploit the roles of the parameters (R_3, R_0, R_1, R_2) in adjusting the yield spread for stochastic volatility. This is illustrated in Figure 9 for the Ford data.

The fitted parameters (R_0, R_1, R_2, R_3) (reported in the Figure captions) are small, validating the use of the asymptotic approximation. Our corrections enable us to match yield spreads for maturities one year and above, compared with only four years and above with the simpler Black-Cox model.

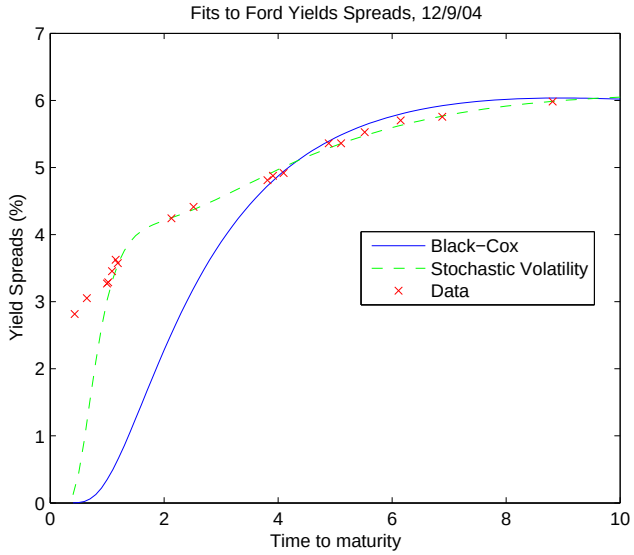

Figure 7: *Black-Cox and two-factor stochastic volatility fits to Ford yield spread data. The short rate is fixed at* $r = 0.025$*. The fitted Black-Cox parameters are* $\bar{\sigma} = 0.35$ *and* $x/B = 2.875$*. The fitted stochastic volatility parameters are* $\sigma^\star = 0.385$*, corresponding to* $R_2 = 0.0129$*,* $R_3 = -0.012$*,* $R_1 = 0.016$ *and* $R_0 = -0.008$*.*

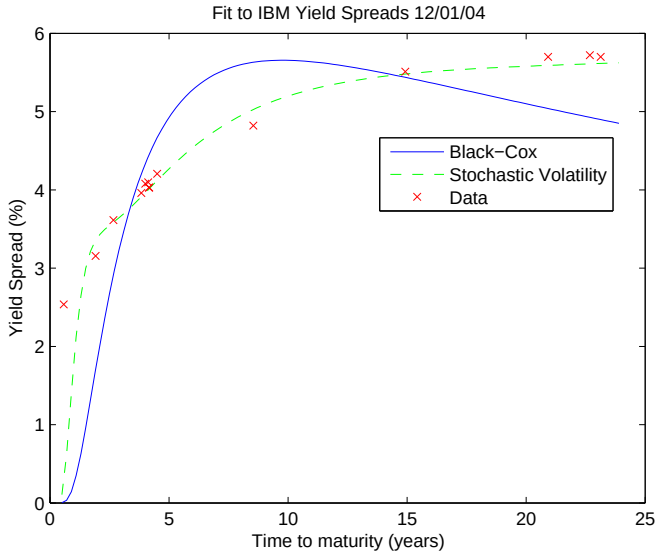

Figure 8: *Black-Cox and two-factor stochastic volatility fits to IBM yield spread data. The short rate is fixed at* $r = 0.025$*. The fitted Black-Cox parameters are* $\bar{\sigma} = 0.35$ *and* $x/B = 3$*. The fitted stochastic volatility parameters are* $\sigma^\star = 0.36$*, corresponding to* $R_2 = 0.00355$*,* $R_3 = -0.0112$*,* $R_1 = 0.013$ *and* $R_0 = -0.0045$*.*

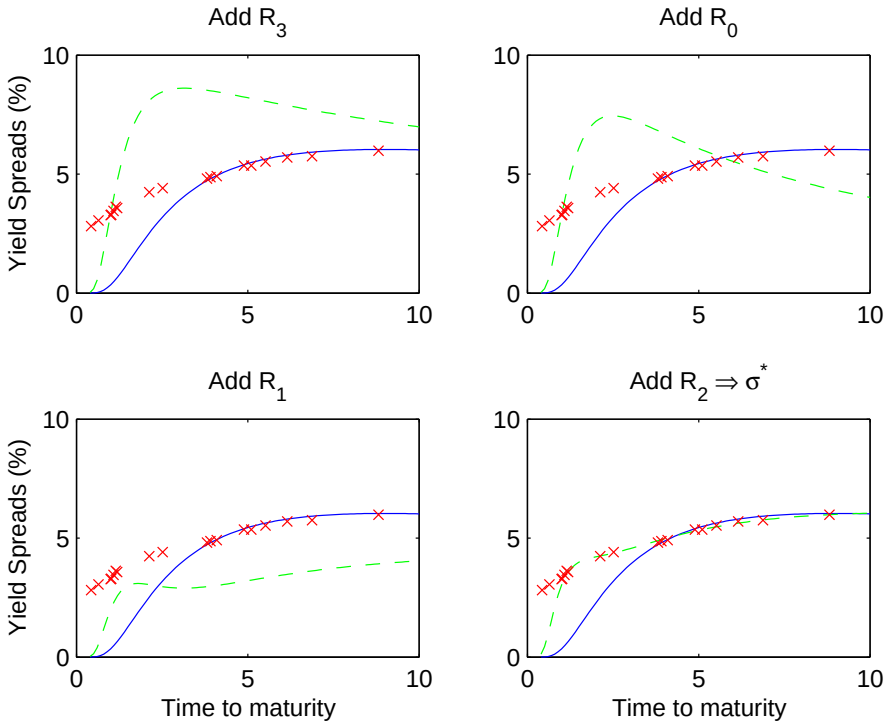

Figure 9: *The effect of introducing the correction parameters successively. The solid curves in each plot show the Black-Cox fit to the Ford data with* $\bar{\sigma} = 0.35$ *and* $x/B = 2.875$*. The top left plot shows that the effect of adding the fast factor skew correction parameterized by* $R_3 = -0.012$ *(with* $R_0 = R_1 = R_2 = 0$*) is to get closer to the short maturity yields. Then the level of the curve at longer maturities is adjusted by bringing in the slow factor level correction parameterized by* $R_0 = -0.008$*. Next, introducing the slow factor skew correction parameterized by* $R_1 = 0.016$ *twists the curve to match the slope at medium to long maturities. Finally, the level of the whole curve is adjusted by* R_2 *(through* $\sigma^\star$*) as shown in the bottom right plot.*

References

[1] T. Bielecki and M. Rutkowski. Credit Risk: Modeling, Valuation an Hedging, *Springer Finance* 2002.

[2] F. Black and J.C. Cox. Valuing corporate securities: Some effects of bond indenture provisions. *Journal of Finance*, **31**:351–367, 1976.

[3] S. Boyarchenko. Endogenous Default under Lévy Processes. Working paper.

[4] P. Collin-Dufresne and R. Goldstein. Do Credit Spreads Reflect Stationary Leverage Ratios? Reconciling Structural and Reduced Form Frameworks. *Journal of Finance* **56**, 1929-1958, 2001.

[5] D. Duffie and K. Singleton. *Credit Risk*. Princeton University Press, 2003.

[6] P. Cotton, J.P. Fouque, G. Papanicolaou and R. Sircar. Stochastic Volatility Corrections for Interest Rates derivatives, *Mathematical Finance* **14**(2), 173-200, 2004.

[7] D. Duffie and D. Lando. Term Structures of Credit Spreads with Incomplete Accounting Information. *Econometrica* **69**, 633-664. 2001.

[8] Y. Eom, J. Helwege, and J.Z. Huang. Structural Models of Corporate Bond Pricing: An empirical Analysis. *Review of Financial Studies* **17**, 499-544. 2004.

[9] J.-P. Fouque, G. Papanicolaou, and R. Sircar. *Derivatives in Financial Markets with Stochastic Volatility*. Cambridge University Press, 2000.

[10] J.-P. Fouque, G. Papanicolaou, R. Sircar, and K. Sølna. Short Time-Scale in S&P 500 Volatility. *Journal of Computational Finance*, **6**(4): 1–23, 2003.

[11] J.-P. Fouque, G. Papanicolaou, R. Sircar and K. Sølna. Singular Perturbations in Option Pricing. *SIAM Journal on Applied Mathematics*, **63**(5), 1648-1665 (2003).

[12] J.-P. Fouque, G. Papanicolaou, R. Sircar and K. Sølna. Multiscale Stochastic Volatility Asymptotics. *SIAM Journal Multiscale Modeling and Simulation*, **2**(1): 22-42, 2004.

[13] J.-P. Fouque, G. Papanicolaou, R. Sircar and K. Sølna. Timing the Smile. *Wilmott Magazine*, March 2004.

[14] K. Giesecke. Correlated default with Incomplete Information. *Journal of Banking and Finance*, **28**(7), 1521-1545, 2004.

[15] K. Giesecke. Default and Information. *Journal of Economic Dynamics and Control*, forthcoming, 2005.

[16] K. Giesecke. Credit Risk Modelling and Valuation: An Introduction. In *Credit Risk, Models and Management* Ed. D. Shimko, 2nd edition, Risk Books, 487-526, 2004.

[17] B. Hilberink and C. Rogers. Optimal Capital Structure and Endogenous Default, *Finance and Stochastics*, **6**(2), 237-263 (2002).

[18] A. Ilhan, M. Jonsson, and R. Sircar, Singular perturbations for boundary value problems arising from exotic options, *SIAM J. Applied Math.*, **64**(4), 1268-1293, 2004.

[19] I. Karatzas and S. Shreve. *Brownian Motion and Stochastic Calculus*, 2nd edition, Springer-Verlag, 1991.

[20] F. Longstaff and E. Schwartz. Valuing Risky Debt: A New Approach. *The Journal of Finance* **50**, 789-821, 1995.

[21] R. Merton. On the pricing of corporate debt: the risk structure of interest rates. *Journal of Finance*, **29**:449–470, 1974.

[22] Ph. Schönbucher. *Credit Derivatives Pricing Models*. Wiley, 2003.

[23] D. Shimko (Editor). *Credit Risk, Models and Management* 2nd edition, Risk Books, 2004.

[24] P. Wilmott, S. Howison, and J. Dewynne. *The Mathematics of Financial Derivatives. A student introduction*. Cambridge University Press, 1995.

[25] C. Zhou. The Term Structure of Credit Spreads with Jump Risk. *Journal of Banking and Finance*, **25**, 2015-2040, 2001.

A Fast Scale Correction Formulas

In this appendix we derive formulas for the function $F_3(t,x)$ and $g(t)$ needed in the fast scale correction presented in Section 4.3. Using the relations

$$\frac{\partial d_2^{\pm}}{\partial x} = \frac{\pm 1}{x\sigma\sqrt{T-t}}\,, \quad N^{''}(z) = -zN^{'}(z)\,,$$

and defining $F_2(t,x) = x^2 \frac{\partial^2 u_0^\star}{\partial x^2}(t,x)$, one obtains successively

$$\begin{aligned} e^{r(T-t)}F_2(t,x) &= N'(d_2^+)\left[-\frac{d_2^+}{(\sigma^\star\sqrt{T-t})^2} - \frac{1}{\sigma^\star\sqrt{T-t}}\right] \\ &+ N'(d_2^-)\left[\frac{d_2^-}{(\sigma^\star\sqrt{T-t})^2} + \frac{2p-1}{\sigma^\star\sqrt{T-t}}\right]\left(\frac{x}{B}\right)^p \\ &+ N(d_2^-)\left[(1-p)p\right]\left(\frac{x}{B}\right)^p, \end{aligned} \tag{55}$$

and

$$
\begin{aligned}
e^{r(T-t)}F_3(t,x) &= N'(d_2^+)\left[\frac{(d_2^+)^2-1}{(\sigma^\star\sqrt{T-t})^3}+\frac{d_2^+}{(\sigma^\star\sqrt{T-t})^2}\right] \\
&+ N'(d_2^-)\left[\frac{(d_2^-)^2-1}{(\sigma^\star\sqrt{T-t})^3}+\frac{(3p-1)d_2^-}{(\sigma^\star\sqrt{T-t})^2}+\frac{p(3p-2)}{\sigma^\star\sqrt{T-t}}\right]\left(\frac{x}{B}\right)^p \\
&+ N(d_2^-)\left[(1-p)p^2\right]\left(\frac{x}{B}\right)^p.
\end{aligned} \tag{56}
$$

At the boundary $x = B$, one has $d_2^+ = d_2^- = d$ defined in (31), and so we deduce formula (30) for g.

B Slow Scale Correction Formulas

In this appendix we derive formulas for the functions $u_{1a}^{(z)}(t,x) + u_{1c}^{(z)}(t,x)$ and $g_d(t)$ needed in the slow scale correction presented in Section 5. Observe that

$$
u_{1a}^{(z)} + u_{1c}^{(z)} = 2(T-t)\left(R_0F_0^{(z)} + R_1F_1^{(z)}\right) - (T-t)^2 f_2(z)\left(R_0F_2^{(z)} + R_1F_3^{(z)}\right), \tag{57}
$$

where $F_2^{(z)}$ and $F_3^{(z)}$ are given in (55) and (56) with $\sigma^\star$ replaced by $f_2(z)$, and $F_0^{(z)}$ and $F_1^{(z)}$ are defined by

$$
F_0^{(z)}(t,x) = \frac{\partial u_{BS}}{\partial \sigma}, \quad F_1^{(z)}(t,x) = x\frac{\partial}{\partial x}\left(\frac{\partial u_0^{(z)}}{\partial \sigma}\right),
$$

and given explicitly by

$$
\begin{aligned}
e^{r(T-t)}F_0^{(z)}(t,x) &= N^{'}(d_2^+)\left[-\frac{d_2^+}{\sigma}-\sqrt{T-t}\right] \\
&+ N^{'}(d_2^-)\left[\frac{d_2^-}{\sigma}+\sqrt{T-t}\right]\left(\frac{x}{B}\right)^p \\
&+ N(d_2^-)\left[\frac{2}{\sigma}(p-1)\log\left(\frac{x}{B}\right)\right]\left(\frac{x}{B}\right)^p,
\end{aligned} \tag{58}
$$

$$
\begin{aligned}
e^{r(T-t)}F_1^{(z)}(t,x) &= N^{'}(d_2^+)\left[\frac{(d_2^+)^2-1}{\sigma^2\sqrt{T-t}}+\frac{d_2^+}{\sigma}\right] \\
&+ N^{'}(d_2^-)\left[\frac{(d_2^-)^2-1}{\sigma^2\sqrt{T-t}}+(1+p)\frac{d_2^-}{\sigma}+p\sqrt{T-t}+\frac{2(1-p)}{\sigma^2\sqrt{T-t}}\log\left(\frac{x}{B}\right)\right]\left(\frac{x}{B}\right)^p \\
&+ N(d_2^-)\left[\frac{2}{\sigma}(p-1)\left(1+p\log\left(\frac{x}{B}\right)\right)\right]\left(\frac{x}{B}\right)^p.
\end{aligned} \tag{59}
$$

At the boundary $x = B$ we have

$$d_2^+ = d_2^- = d \quad = \quad -\frac{pf_2(z)\sqrt{T-t}}{2},$$

and the function $g_d(t)$ defined by

$$g_d(t) = -\lim_{x \downarrow B} \left(u_{1a}^{(z)}(t,x) + u_{1c}^{(z)}(t,x) \right),$$

is therefore expressed as

$$g_d(t) = -2(T-t)\left(R_0 F_0^{(z)}(t,B) + R_1 F_1^{(z)}(t,B) \right) + (T-t)^2 f_2(z)\left(R_0 F_2^{(z)}(t,B) + R_1 F_3^{(z)}(t,B) \right). \quad (60)$$